

$^{29,30}\text{Si}(^{16}\text{O}, ^{15}\text{N})$ proton stripping reaction at 60 MeV*

D. Dehnhard, J. L. Artz, D. J. Weber, and V. Shkolnik

Williams Laboratory of Nuclear Physics, University of Minnesota, Minneapolis, Minnesota 55455

R. M. DeVries

Nuclear Structure Laboratory, University of Rochester, Rochester, New York 14627

(Received 7 July 1975)

Differential cross sections of the [$^{16}\text{O}, ^{15}\text{N}(\text{g.s.})$] reaction on ^{29}Si and ^{30}Si were measured at $E(^{16}\text{O}) = 60$ MeV at far forward angles. The strongly oscillatory $\Delta L = 1, (2)$ angular distributions for the $2s_{1/2}$ and $1d_{3/2}$ transitions to ^{30}P and ^{31}P were found to be out of phase. The pure $\Delta L = 1, 2s_{1/2}$ transitions were fitted well by finite range distorted wave Born approximation calculations using the code LOLA. The phase of the structure of the $1d_{3/2}$ transfer angular distributions could not be fitted with the distorted wave Born approximation. Spectroscopic factors were in good agreement with ($^3\text{He}, d$) results for $2s_{1/2}$ and $1d_{5/2}$ transitions and a factor of 2 too large for $1d_{3/2}$ transfer. This factor of 2 for the $1d_{3/2}$ transitions is not understood. The mixed j transition to the 2^+ state in ^{30}P (1.454 MeV) was found to be consistent with almost exclusive $j = \frac{3}{2}$ transfer as predicted by shell model calculations.

$$\left[\text{NUCLEAR REACTIONS } ^{29,30}\text{Si}(^{16}\text{O}, ^{15}\text{N}), E = 60 \text{ MeV; measured } \sigma(E_{^{15}\text{N}}, \theta), \right. \\ \left. \text{deduced } C^2S_{ij}. \right]$$

I. INTRODUCTION

In a direct single particle transfer reaction on even-even targets the spin J_f of the residual nucleus is equal to the j value of the orbital into which the particle is transferred. If the target is odd-even, usually several orbitals with different j values between $|J_f - J_i|$ and $J_f + J_i$ can contribute to the transition, where J_i is the target spin. For example, if the target has $J_i^\pi = \frac{1}{2}^+$, a $J_f^\pi = 2^+$ can be reached by transfer of either $j_c = \frac{3}{2}^+$ or $j_s = \frac{5}{2}^+$. For comparison with shell model calculations a knowledge of the relative amounts of j_c and j_s transfer is of particular interest.

The angular distributions of (d, p) or similar light ion induced reactions with unpolarized beams do not show sufficient j dependence to allow an extraction of the individual j_c and j_s transfer strengths. Usually, the analysis is done with the assumption that either of the two j values is dominant. In heavy ion induced transfer reactions, however, the transitions with the j_s transfer are strongly enhanced^{1,2} over the ones with the j_c transfer. This enhancement should make it possible to measure, for example, the strength of a weak $1d_{5/2}$ component in the presence of a strong $1d_{3/2}$ component. The enhancement of the j_s transitions is a consequence of angular momentum selection rules and matching conditions.³

The orbital angular momentum transfer ΔL is restricted by the two conditions

$$|l_1 - l_2| \leq \Delta L \leq l_1 + l_2$$

and

$$|j_1 - j_2| \leq \Delta L \leq j_1 + j_2.$$

For stripping reactions l_1 and j_1 and l_2 and j_2 are orbital and total angular momenta of the transferred particle in the projectile (1) and residual nucleus (2), respectively. Specifically, for the proton transfer reaction [$^{16}\text{O}, ^{15}\text{N}(\text{g.s.})$] we have $l_1 = 1$ and $j_1^\pi = \frac{1}{2}^-$ so that a transfer to an $l_2 = 2$ and $j_2^\pi = \frac{3}{2}^+$ orbit can proceed by $\Delta L = 1$ and 2, and a transfer to an $l_2 = 2$ and $j_2^\pi = \frac{5}{2}^+$ orbit can proceed by $\Delta L = 2$ and 3. Brink's³ matching conditions are mostly closely satisfied for $\Delta L = 3$ for the ($^{16}\text{O}, ^{15}\text{N}$) reaction on ^{29}Si and ^{30}Si at 60 MeV, the subject of the present investigation. Consequently, the cross section for a $\Delta L = 3$ transition is expected to be considerably larger than the one for a $\Delta L = 1$ transition of equal spectroscopic strength. A summary of these allowed orbital angular momentum transfers for transitions to the shell model orbits of interest in the ($^{16}\text{O}, ^{15}\text{N}$) reaction on ^{30}Si and ^{29}Si is given in Table I along with the respective g.s. Q values, excitation energies, and J_f values of the final states in the residual nucleus.⁴ The normal ΔL is underlined in the table. The relatively weak nonnormal $\Delta L = 2$ recoil term contributes to the angular distribution significantly only at the minima of the normal $\Delta L = 1$ angular distribution, both angular distributions being out of phase with each other.

An experimental estimate for the enhancement of the j_s transition over the j_c transition can be obtained from a comparison of the ($^{16}\text{O}, ^{15}\text{N}$) and ($^3\text{He}, d$) reactions on the even-even ^{30}Si target.⁵⁻⁸ We have chosen ^{30}Si as a target rather than ^{28}Si

TABLE I. Basic data (Ref. 4) of the reactions studied.

Reaction ^a	Q (MeV)	E_x (MeV)	J^π	$n_2 l_2 j_2$ ^b	ΔL ^c
$^{30}\text{Si}(^{16}\text{O}, ^{15}\text{N})^{31}\text{P}$	-4.830	0.0	$\frac{1}{2}^+$	$2s_{1/2}$	<u>1</u>
		1.266	$\frac{3}{2}^+$	$1d_{3/2}$	<u>1</u> , 2
		2.234	$\frac{5}{2}^+$	$1d_{5/2}$	2, <u>3</u>
$^{29}\text{Si}(^{16}\text{O}, ^{15}\text{N})^{30}\text{P}$	-6.528	0.0	1^+	$2s_{1/2}$	<u>1</u>
				$(1d_{3/2})$	(<u>1</u> , 2)
		1.454	2^+	$1d_{3/2}$	<u>1</u> , 2
				$(1d_{5/2})$	(2, <u>3</u>)
	1.973	3^+	$1d_{5/2}$	2, <u>3</u>	

^a Only ^{15}N (g.s.) with $(n_1 l_1 j_1) = (1p_{1/2})$ was observed.

^b $(n_2 l_2 j_2)$ of orbitals which contribute only weakly are in parentheses.

^c Normal ΔL are underlined.

because the very negative Q value, -9.380 MeV for $^{28}\text{Si}(^{16}\text{O}, ^{15}\text{N})^{29}\text{P}$ (g.s.), implies very poor matching in this latter reaction.

In the $^{29}\text{Si}(^{16}\text{O}, ^{15}\text{N})^{30}\text{P}$ reaction, the transition to the 2^+ state at 1.454 MeV is of particular interest, because shell model calculations predict⁹ a small $1d_{5/2}$ component for the transition to this state in addition to a strong $1d_{3/2}$ component. The major objective of this experiment is to measure the small $1d_{5/2}$ component in this heavy ion induced transfer reaction.

II. EXPERIMENTAL PROCEDURE

A 60 MeV ^{16}O beam was supplied by the University of Minnesota MP tandem Van de Graaff. A duoplasmatron source in combination with a CH_4 exchange gas was used to generate $^{16}\text{O}^-$ ions. Targets were self-supporting SiO_2 foils, typically $50 \mu\text{g}/\text{cm}^2$ thick, with isotopic enrichments of 92% for ^{29}Si and 95.6% for ^{30}Si . Two pairs of 30 mm long, 10 mm high, position sensitive solid state detectors were placed along the focal plane of an Enge split-pole spectrometer to detect both ^{15}N (6^+) and ^{15}N (7^+) ions simultaneously. These two charge states are of comparable intensity at the outgoing energies of the present experiment while the fraction¹⁰ of ^{15}N (5^+) ions is less than 5%. It was necessary to detect both the 6^+ and the 7^+ charge states because the self-supporting target foils would not generate the equilibrium charge state fractions. In elastic scattering experiments it was observed that the charge state fractions would asymptotically reach the values for charge state equilibrium due to the slow carbon buildup on the target.

Particle identification was accomplished by

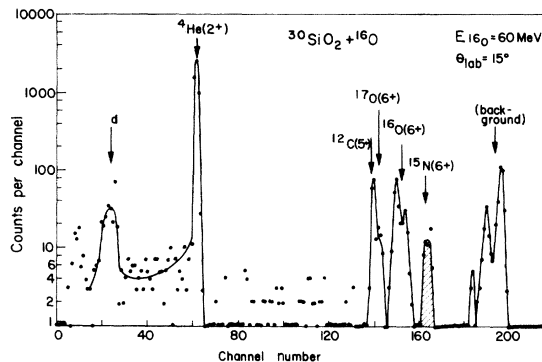


FIG. 1. Energy spectrum for one position solid state detector used for ^{15}N (6^+) ion identification in the $^{30}\text{Si}(^{16}\text{O}, ^{15}\text{N})^{31}\text{P}$ reaction.

measuring the energy of the ions which, for the same magnetic rigidity, is proportional to Z^2/M where Z is the charge and M is the mass of the ion. This is possible because over the 30 mm length of a single detector the magnetic rigidity is sufficiently constant. A typical energy spectrum is shown in Fig. 1. The position signals (X), generated by dividing the (XE) signal of the detector by the (E) signal, were accumulated with gates set on the groups corresponding to the ^{15}N (6^+) ions for one pair of detectors and to the ^{15}N (7^+) ions for the other pair. Position (X) spectra obtained with two adjacent detectors are shown in Fig. 2 for the $^{29}\text{Si}(^{16}\text{O}, ^{15}\text{N})^{30}\text{P}$ reaction at $\theta_{\text{lab}} = 20^\circ$. The over-all resolution width of 70 keV is due mainly to target thickness.

Differential cross sections were measured in 1.25° steps from $\theta_{\text{lab}} = 5^\circ$ to 25° on ^{29}Si and ^{30}Si , and in 0.5° steps from $\theta_{\text{lab}} = 3.5^\circ$ to 5° on ^{29}Si . They are shown in Figs. 3 and 4 together with the results of distorted wave Born approximation (DWBA) calculations to be discussed later. The angular acceptance of the spectrometer was set to 1° , corresponding to a solid angle of ~ 0.9 msr. Two

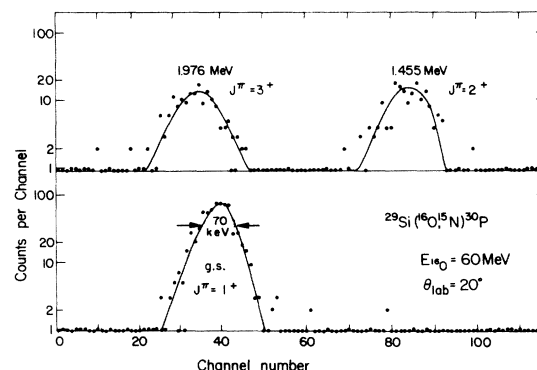


FIG. 2. Position ($X=XE/E$) spectra of ^{15}N (6^+) ions for two adjacent detectors in the $^{29}\text{Si}(^{16}\text{O}, ^{15}\text{N})^{30}\text{P}$ reaction.

monitor detectors, placed at $\theta_{\text{lab}} = \pm 30^\circ$ with respect to the beam, were used to detect elastically scattered ^{16}O ions to check for possible target deterioration effects. Absolute cross sections to an accuracy of 15% were derived from a best optical model fit to the yields of elastically scattered ^{16}O ions using the code RAROMP.¹¹ The cross section errors given in Figs. 3 and 4 are relative errors only, derived from the statistical accuracy and the reproducibility of the data and do not include the above given error of the absolute cross sections. Relative errors not explicitly shown lie within the size of the data points.

III. EXPERIMENTAL ANGULAR DISTRIBUTIONS AND DWBA CALCULATIONS

A. $^{30}\text{Si}(^{16}\text{O}, ^{15}\text{N})^{31}\text{P}$

Angular distributions for the $^{30}\text{Si}(^{16}\text{O}, ^{15}\text{N})^{31}\text{P}$ reaction are shown in Fig. 3. Rather large oscillations are observed in particular for the ground state (g.s.) transition. Surprisingly, the transitions to the $\frac{1}{2}^+$ g.s. and the $\frac{3}{2}^+$ first excited state are found to be out of phase even though both transitions proceed by $\Delta L = 1$ in the no-recoil

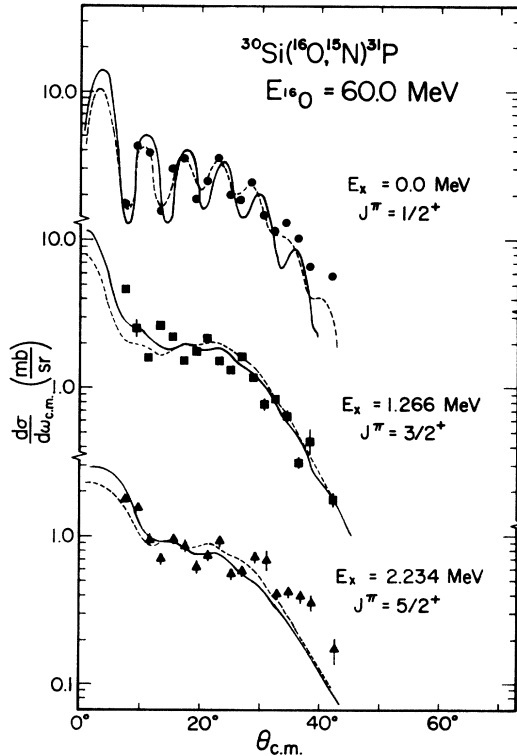


FIG. 3. Experimental angular distributions for the $^{30}\text{Si}(^{16}\text{O}, ^{15}\text{N})^{31}\text{P}$ reaction together with DWBA curves. Solid lines: optical model parameter set 1. Broken lines: set 2.

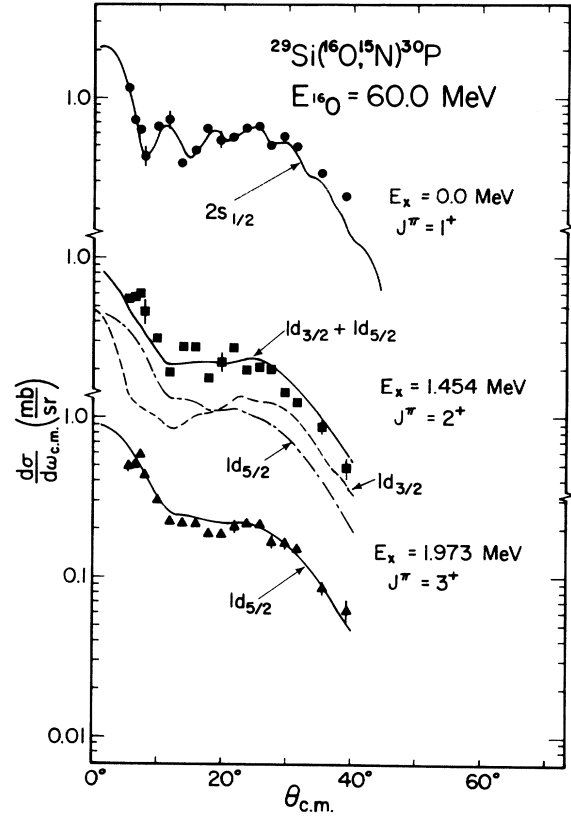


FIG. 4. Experimental angular distributions for the $^{29}\text{Si}(^{16}\text{O}, ^{15}\text{N})^{30}\text{P}$ reaction and DWBA curves using optical model parameter set 1.

approximation (see Table I).

The curves shown in Fig. 3 (and in Fig. 4 to be discussed later) are the results of calculations done with the finite range DWBA code LOLA¹² which includes recoil exactly. The optical model parameters used in these calculations are given in Table II. Set 1 was obtained by fitting the $^{16}\text{O} + ^{32}\text{S}$ data of Ref. 13. Set 2 has been used previously¹⁴ for DWBA calculations for the $\text{Si}(^{16}\text{O}, ^{15}\text{N})$ reaction. Bound states were calculated in Woods-Saxon wells of $r = 1.25$ fm and $a = 0.65$ fm using the known binding energy and a Thomas-Fermi spin orbit strength $\lambda = 20.0$.

TABLE II. Optical model parameters used for both entrance and exit channels.

Set	V (MeV)	r_r^a (fm)	a_r (fm)	W_V (MeV)	r_i^a (fm)	a_i (fm)	r_c^a (fm)
1	23.6	1.35	0.467	12.6	1.27	0.255	1.35
2 ^b	100.0	1.14	0.68	20.0	1.20	0.60	1.35

^a Potential radii $R = r(A_1^{1/3} + A_2^{1/3})$.

^b Reference 14.

Both optical parameter sets used in the calculations of Fig. 3 yield good fits to the $2s_{1/2}$ g.s. transition [the fit with set 2 being slightly better for ^{31}P ($\frac{1}{2}^+$)], but both fail to reproduce the shape of the $1d_{3/2}$ state angular distribution. Surprisingly, use of the parameter set 2 yields calculated cross sections a factor of two smaller than set 1. This will be discussed in more detail in the next chapter. We were unable to find a modified parameter set which would fit the $1d_{3/2}$ state angular distribution. The calculated $\Delta L=2$ recoil contribution for the $\frac{3}{2}^+$ transition is out of phase with the $\Delta L=1$ component and would fit the $\frac{3}{2}^+$ angular distribution very well; however, the calculated total $\Delta L=2$ cross section is an order of magnitude smaller than the normal $\Delta L=1$ contribution. A similar anomaly, i.e., data in phase with DWBA calculations using the (weaker) nonnormal ΔL angular distribution, has been seen before.^{15, 16} The calculation for the $\frac{3}{2}^+$ state of ^{31}P (2.234 MeV) reproduces the gross features of the data but is unable to account for the observed fine structure.

As mentioned previously, both the g.s. ($\frac{1}{2}^+$) and the 1.266 MeV ($\frac{3}{2}^+$) state should involve $\Delta L=1$ transitions with a small, nearly negligible, $\Delta L=2$ recoil component for the $1d_{3/2}$ transition. Interestingly, the two DWBA predictions for the two states were very different in shape, as shown in Fig. 3. We found that this difference is due to a number of effects. The binding energies E_B and Q values differ, resulting in a damping of the oscillations for the excited state. This effect is discussed further in the comparison of the ^{30}P and ^{31}P g.s. transitions. The effect of different angular momentum coupling is of greater interest; i.e., the $1d_{3/2}$ transition involves transferring the $l_1=1$ proton in ^{16}O to an $l_2=2$ orbit in ^{31}P while the $2s_{1/2}$ transition involves transfer to an $l_2=0$ orbit. For the $1d_{3/2}$ transfer this results in a vastly greater number of possible angular momentum couplings (angular momentum tensors of Ref. 12) which also damps the predicted angular distribution for the first excited state. Figure 5 shows three calculated curves using a $2s_{1/2}$ radial form factor throughout. The solid line gives the normal calculation for the $2s_{1/2}$ g.s. transition. The broken line shows the effect of the change in E_B and Q only; again a $2s_{1/2}$ transfer is assumed. The dash-dot line finally was obtained by use of the g.s. E_B and Q and $2s_{1/2}$ radial form factor, but allowing for the angular momentum couplings of a $1d_{3/2}$ transfer by an appropriate modification of the code. It is quite clear that the $1d_{3/2}$ coupling has a considerably larger damping effect than the change in E_B and Q . However, the $1d_{3/2}$ coupling caused a shift in the calculated diffraction pattern towards smaller angles, while a shift towards

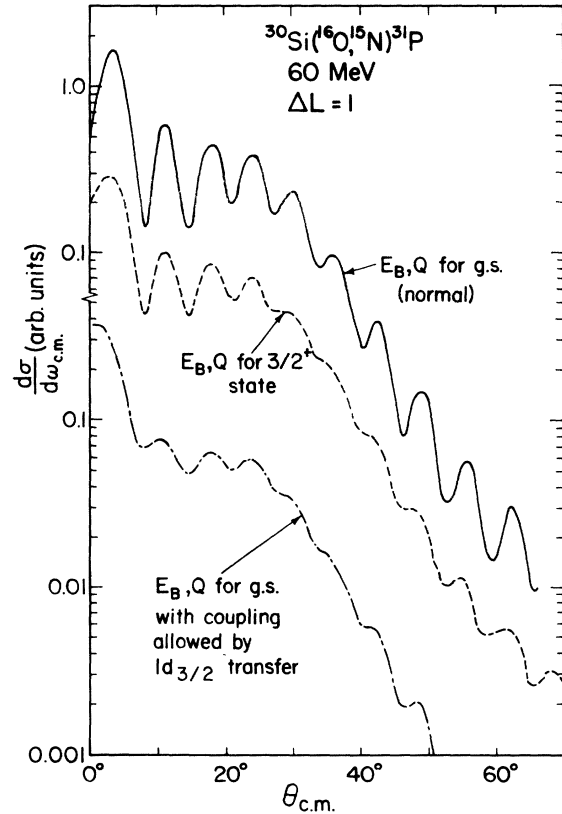


FIG. 5. Q -value and angular momentum coupling effects in DWBA calculations for a pure $\Delta L=1$ transition. All curves shown were calculated utilizing a $2s_{1/2}$ radial form factor.

larger angles is necessary to fit the shape of the experimental angular distribution for the $\frac{3}{2}^+$ state. The normal calculation for the $1d_{3/2}$ transfer state gives essentially the same shape as the dash-dot line of Fig. 5.

B. $^{29}\text{Si}(^{16}\text{O}, ^{15}\text{N})^{30}\text{P}$

Angular distributions for the $^{29}\text{Si}(^{16}\text{O}, ^{15}\text{N})^{30}\text{P}$ reaction are shown in Fig. 4 for the $J^\pi=1^+$ ground state, the 2^+ state at 1.454 MeV, and the 3^+ state at 1.973 MeV. The 0^+ and 1^+ doublet at ~ 0.7 MeV could not be resolved. No angular distribution was taken, since for most runs the doublet fell between the two detectors on the focal plane.

The data for the 1^+ g.s. are nearly in phase with those for the pure $\Delta L=1$, g.s. transition in the $^{30}\text{Si}(^{16}\text{O}, ^{15}\text{N})^{31}\text{P}$ reaction although the oscillations are not as pronounced as for the ^{30}Si target. The 1^+ state in ^{30}P can be reached both by $2s_{1/2}$ and $1d_{3/2}$ transfer. However, the ($^3\text{He}, d$) and (d, n) experiments¹⁷⁻¹⁹ showed almost pure $2s_{1/2}$ transfer in agreement with shell model calculations.⁹ Thus, the $^{29}\text{Si}(^{16}\text{O}, ^{15}\text{N})^{30}\text{P}$ (g.s.) transi-

tion may be taken as another example for a $2s_{1/2}$, $\Delta L=1$ angular distribution. In fact, the observed damping of the oscillations, compared to ^{30}Si -(^{16}O , ^{15}N) ^{31}P (g.s.), was correctly reproduced by DWBA calculations and appears to be a Q -value effect.

It should be emphasized at this point that the difference in Q values between the two $2s_{1/2}$ g.s. transitions to ^{30}P and ^{31}P is larger than the difference in Q values between the g.s. and first excited state in ^{31}P . The striking difference in shape between the experimental $2s_{1/2}$ and $1d_{3/2}$ transitions of ^{31}P thus cannot only be due to a difference in Q values. The same conclusion was reached from the DWBA calculations shown in Fig. 5.

According to Table I, the 2^+ state of ^{30}P (1.454 MeV) can be reached either by $1d_{3/2}$ or $1d_{5/2}$ transfer or both. The experimental angular distribution for the 2^+ state transition exhibits a shape very similar to that of the pure $1d_{3/2}$ transition to ^{31}P (1.266 MeV). We are tempted to use this fact as evidence for a principal $1d_{3/2}$ component in the transition to this 2^+ state. However, the structure of the experimental angular distribution for the $\frac{5}{2}^+$ state ($\Delta L=3$) is also not very different from that of the 2^+ state. Thus, at this energy, it is very difficult to derive the angular momentum of the transferred particle from the shape of the angular distributions.²⁰ Furthermore, calculated $1d_{3/2}$ transfer angular distributions for ^{30}Si (^{16}O , ^{15}N) ^{31}P ($\frac{3}{2}^+$) and ^{29}Si (^{16}O , ^{15}N) ^{30}P (2^+) of Figs. 3 and 4, respectively, show much larger differences in shape than observed experimentally. The calculation for the former reaction fits the general shape of the experimental distribution quite well but the observed oscillations are out of phase with the strongly damped oscillation in the calculations. [Figure 5 shows a $1d_{3/2}$ angular distribution (dash-dot line) with stronger oscillations because the $\Delta L=2$ recoil term was not included.] The $1d_{3/2}$ calculation for the latter reaction [^{29}Si (^{16}O , ^{15}N) ^{30}P (2^+)] fails to fit the forward angle data when normalized at the grazing angle (Fig. 4, dashed line).

The angular distribution for the transition to the 3^+ state (1.973 MeV) which can go only by $1d_{5/2}$ transfer (if we restrict ourselves to the $2s1d$ shell) is smoother than that for the $\frac{5}{2}^+$ state in ^{31}P and is fitted very well by DWBA.

IV. SPECTROSCOPIC FACTORS

Despite the still unsolved problem of fitting the details of the shape of the $1d_{3/2}$ angular distribution by the DWBA, we proceed to extract products of spectroscopic factors $C_1^2 S_1 \times C_2^2 S_2$ from the data. Spectroscopic factors $C_2^2 S_2$ for proton strip-

TABLE III. Spectroscopic factors $C_2^2 S_2$ for proton transfer to ^{31}P states.

E_x	J^π	$C_2^2 S_2$ from (^3He , d)					$C_2^2 S_2$ from (^{16}O , ^{15}N)		$C_2^2 S_2$ Shell model ^j		
		12 MeV ^a	15 MeV ^b	17.85 MeV ^c	25 MeV ^d	42 MeV ^e	42 MeV ^f	45 MeV ^g		73.5 MeV ^h	60 MeV ⁱ
0.0	$\frac{1}{2}^+$	0.47	0.44	0.5	0.52	0.5	0.7	(0.5)	0.56	0.61	0.65
1.266	$\frac{3}{2}^+$	0.48	0.80	0.65	0.57	2.5	1.3	1.9	0.74	1.2	0.52
2.234	$\frac{3}{2}^+$	0.05	0.08	0.13	0.09	0.09	0.13	***	0.30	0.10	0.04

^a Reference 5.

^b Reference 6.

^c Reference 7.

^d Reference 8.

^e Reference 23, analyzed without recoil and an optical model parameter set similar to set 2 (Table II).

^f Data of Ref. 23, analyzed in the present work with recoil and parameter set 1 (Table II). The renormalization of the data of Ref. 23 as claimed in Ref. 24 appears not necessary.

^g Reference 25, without recoil. Here absolute $C_2^2 S_2$ for g.s. transition is normalized to 0.5.

^h Reference 14, an " S_1 " = 3.5 was used in Ref. 14 instead of the appropriate $C_1^2 S_1 = 1.75$, i.e., values in this column should be multiplied by 2.

ⁱ This experiment.

^j Reference 22.

ping onto Si were obtained by dividing out a $C_1^2 S_1 = 1.75$ for $1p_{1/2}$ proton pickup²¹ from ^{16}O . (The isobaric spin Clebsch-Gordan coefficients are $C_1^2 = \frac{1}{2}$ and $C_2^2 = \frac{2}{3}$ for $^{30}\text{Si} \rightarrow ^{31}\text{P}$ and $C_2^2 = \frac{1}{2}$ for $^{29}\text{Si} \rightarrow ^{30}\text{P}$.) We found that the well-fitted($^{16}\text{O}, ^{15}\text{N}$) angular distributions for the g.s. transitions in ^{30}P and ^{31}P give absolute spectroscopic factors in excellent agreement with the ($^3\text{He}, d$) results^{5-8, 17-19} and shell model calculations^{9, 22} when optical model set 1 is used (see Tables III and IV). When extracted from the average cross sections, the spectroscopic factor for the poorly fitted $1d_{3/2}$ transition to ^{31}P is a factor of 2 too large in comparison to the ($^3\text{He}, d$) results or the shell model prediction.²² As can be seen in Table III, which includes results from lower energy ($^{16}\text{O}, ^{15}\text{N}$) data which were analyzed without²³ and with recoil (this work), the effects from recoil are large for this j_π transition. However, if recoil is included and the same optical model set is used, the 42 and 60 MeV results show surprisingly good agreement, but both yield $C_2^2 S_2$ values for $1d_{3/2}$ transfer a factor of 2 larger than from ($^3\text{He}, d$). The discrepancy for the $1d_{5/2}$ transition between all transfer data^{5-8, 23-25} and the shell model value is not to be taken as serious, because it is a weak transition into the "filled" $1d_{5/2}$ shell. Only the $C_2^2 S_2$ value for $^{30}\text{Si}(^{16}\text{O}, ^{15}\text{N})^{31}\text{P}(\frac{3}{2}^+)$ at 73.5 MeV¹⁴ appears to stand out as unusually large among the experimental spectroscopic factors.

Special care has to be taken when comparing spectroscopic factors given by different authors. For example, no spin-orbit term is used in the bound state calculations of Ref. 14. Its inclusion for the Si + p bound state will increase the $1d_{3/2}$ strength and decrease the $1d_{5/2}$ strength. All three ($2s_{1/2}$, $1d_{3/2}$, and $1d_{5/2}$) absolute $C^2 S$ will be affected through the $^{16}\text{O} - ^{15}\text{N} + p$ bound state spin-orbit term. Another difference is that our calculations include the Coulomb part in the inter-

action which causes the transitions. Inclusion of this term reduces considerably the post-prior discrepancy²⁶ and decreases deduced $C_2^2 S_2$ values by 20 to 30%. Further, we use a $C_1^2 S_1 = 1.75$ for proton pickup²¹ from ^{16}O while Ref. 14 used 3.5 because of an apparent mixup between $C^2 S$ and S . That means the " S_2 " values ($C_2^2 S_2$ in our notation) extracted from the 73.5 MeV data have to be multiplied by $C_1^{-2} = 2$. With that factor included, we have a factor of 2 discrepancy in the g.s. transition strength between the 73.5 MeV results¹⁴ and our values. This, however, is a consequence of the use of optical parameter set 2 of Table I which was applied in Ref. 14. Thus, use of this set 2 does yield $C^2 S$ values from our data a factor of 2 larger than those given in Table II, which were obtained with set 1. Consequently, there is no discrepancy between the results of Ref. 14 for the $2s_{1/2}$ transition (after correction for the C_2^2 value) and ours when parameter set 2 is used in both analyses. The factor of 3 discrepancy in the $\frac{5}{2}^+$ (2.234 MeV) state transition between the 73.5 MeV data and our data is obviously too large to be solely due to the bound state spin-orbit term and is not understood. It should also be mentioned that the S_2 values of Refs. 5 and 6 apparently were taken in Ref. 14 as " S_2 " = $C_2^2 S_2$ values without properly inserting the $C_2^2 = \frac{2}{3}$.

If we ignore for the time being the special problems of the $1d_{3/2}$ transitions [no detailed fit of the oscillations and the factor of 2 discrepancy in spectroscopic factors in comparison to ($^3\text{He}, d$)], we may proceed to untangle the mixed $j_2 = \frac{3}{2}^+, \frac{5}{2}^+$ transition to the 2^+ state of ^{30}P . If we assume a pure $\frac{5}{2}^+$, $\Delta L = 3$ transition we get a good fit to the general shape of the 2^+ state angular distribution, and extract a $C_2^2 S_2 = 0.1$, more than two times *smaller* than for a pure $1d_{5/2}$ in ($^3\text{He}, d$) which gave $C_2^2 S_2 = 0.24$. If we assume a pure $\frac{3}{2}^+$, $\Delta L = 1$ transition we have a very poor fit to the

TABLE IV. Spectroscopic factors $C_2^2 S_2$ for proton transfer to ^{30}P states.

E_x	J^π	j_2^π	($^3\text{He}, d$) 15 MeV ^a	($^3\text{He}, d$) 25 MeV ^b	(d, n) 8 MeV ^c	($^{16}\text{O}, ^{15}\text{N}$) 60 MeV ^d	Shell model ^e
0.0	1^+	$\frac{1}{2}^+$	0.48	0.49	0.47	0.61	0.61
1.454	2^+	$\frac{3}{2}^+$	0.33	0.32 ^f	0.34	0.54	0.32
		$\frac{5}{2}^+$...	(0.24) ^f	...	0.05	0.03
1.973	3^+	$\frac{5}{2}^+$	0.22	0.034	0.06	0.10	0.07

^a Reference 17.

^b Reference 18.

^c Reference 19.

^d This experiment.

^e Reference 9.

^f If transition were purely $1d_{3/2}$ or $1d_{5/2}$, respectively.

experimentally observed shape and get a rough estimate for a $1d_{3/2}$ spectroscopic factor $C_2^2S_2 = 1.0$, about a factor of 3 *larger* than for a pure $1d_{3/2}$ in ($^3\text{He}, d$) which gave $C_2^2S_2 = 0.32$. This factor is more than the factor of 2 which we left unexplained in the pure $1d_{3/2}$ transition to the $\frac{3}{2}^+$ state in ^{31}P . Finally, if we consider a mixture of $\frac{3}{2}^+$ and $\frac{5}{2}^+$ transitions, a $1d_{5/2}$ component with a small $C_2^2S_2 \cong 0.05$ added to a $1d_{3/2}$ component with $C_2^2S_2 = 0.54$ gives a good over-all fit to the 2^+ differential cross section, with spectroscopic factors in very good agreement with the shell model prediction.⁹ The small $\frac{5}{2}^+$ strength has a strong effect on the cross section because of the large enhancement of the $j_>$ transition over the $j_<$ transition. It is also very important for the fit at forward angles. The strength of the $1d_{3/2}$ component is larger than the ($^3\text{He}, d$) value by about the same factor as for the

$\frac{3}{2}^+$ state transition in ^{31}P .

In conclusion, the fact that the angular distributions for both the 2^+ state of ^{30}P at 1.454 MeV and the $\frac{3}{2}^+$ state of ^{31}P at 1.266 MeV are out of phase with their respective ground states has not, at present, been explained. This observation and the dependence of absolute spectroscopic factors on different optical model sets require appropriate qualification of the reliability of the extracted $C_2^2S_2$ values. Acknowledging these qualifications, in certain cases the ($^{16}\text{O}, ^{15}\text{N}$) reaction appears to be a useful way in untangling states of mixed j transitions.

ACKNOWLEDGMENT

The authors are indebted to Mr. M. Franey for adapting the LOLA code to the CYBER 74 computer at the University of Minnesota.

*Work supported by the U. S. Energy Research and Development Administration and the National Science Foundation. This is Report No. COO-1265-165.

¹A. R. Barnett, W. R. Phillips, P. J. A. Buttle, and L. J. B. Goldfarb, Nucl. Phys. **A176**, 321 (1971).

²D. G. Kovar, F. D. Becchetti, B. G. Harney, F. Pühlhofer, J. Mahoney, D. W. Miller, and M. S. Zisman, Phys. Rev. Lett. **29**, 1023 (1972).

³D. M. Brink, Phys. Lett. **40B**, 37 (1972).

⁴P. M. Endt and C. van der Leun, Nucl. Phys. **A214**, 1 (1973).

⁵A. C. Wolff and H. G. Leighton, Nucl. Phys. **A140**, 319 (1970).

⁶R. A. Morrison, Nucl. Phys. **A140**, 97 (1970).

⁷H. F. Lutz, D. W. Heikinen, W. Bartolini, and T. H. Curtis, Phys. Rev. C **2**, 981 (1970).

⁸W. W. Dykoski and D. Dehnard, J. H. Williams Laboratory Annual Report, 1971, University of Minnesota (unpublished).

⁹B. H. Wildenthal (private communication) (also quoted in Ref. 19).

¹⁰J. B. Marion and F. C. Young, *Nuclear Reaction Analysis* (North-Holland, Amsterdam, 1968).

¹¹G. J. Pyle, J. H. Williams Laboratory Informal Report No. COO-1265-64, University of Minnesota (unpublished).

¹²R. M. DeVries, Phys. Rev. C **8**, 951 (1973).

¹³P. Braun-Munzinger, W. Bohne, G. K. Gelbke, W. Grochulski, H. L. Harney, and H. Oeschler, Phys. Rev. Lett. **31**, 1423 (1973).

¹⁴I. Tserruya, W. Bohne, P. Braun-Munzinger, C. K. Gelbke, W. Grochulski, H. L. Harney, and J. Kuzminski, Nucl. Phys. **A242**, 345 (1975).

¹⁵R. M. DeVries, M. S. Zisman, J. G. Cramer, K.-L. Liu, F. D. Becchetti, B. G. Harvey, H. Homeyer, D. G. Kovar, J. Mahoney, and W. von Oertzen, Phys. Rev. Lett. **32**, 680 (1974).

¹⁶P. D. Bond, J. D. Garrett, O. Hansen, S. Kahana, M. J. LeVine, and A. Z. Schwarzschild, in *Proceedings of the International Conference on Reactions between Complex Nuclei, Nashville, Tennessee, 1974*, edited by R. L. Robinson, F. K. McGowan, J. B. Ball, and J. H. Hamilton (North-Holland, Amsterdam/American Elsevier, New York, 1974), Vol. I, p. 55.

¹⁷R. C. Hertzog, L. L. Green, M. W. Greene, and G. D. Jones, J. Phys. A: Math., Nucl. Gen. **7**, 72 (1974).

¹⁸W. W. Dykoski and D. Dehnard, Phys. Rev. (to be published).

¹⁹J. Uzureau, D. Ardouin, P. Avignon, A. Adam, and B. Duchemin, Nucl. Phys. **A230**, 253 (1974).

²⁰W. Henning, D. G. Kovar, J. R. Erskine, and L. R. Greenwood, Phys. Lett. **55B**, 49 (1975).

²¹H. W. Fulbright, J. A. Robbins, M. Blann, D. G. Fleming, and H. S. Plendl, Phys. Rev. **184**, 1068 (1969).

²²B. H. Wildenthal, J. B. McGrory, E. C. Halbert, and H. D. Graber, Phys. Rev. C **4**, 1708 (1971).

²³T. J. Lewis, G. H. Wedberg, J. C. Peng, J. L. Ricci, C. M. Cheng, and J. V. Maher, Phys. Rev. C **8**, 678 (1973).

²⁴R. M. DeVries, Phys. Rev. C **8**, 1542 (1973).

²⁵J. B. Ball, O. Hansen, J. S. Larsen, D. Sinclair, and F. Videbaeck, Phys. Lett. **49B**, 348 (1974).

²⁶R. M. DeVries, G. R. Satchler, and J. G. Cramer, Phys. Rev. Lett. **32**, 1388 (1974).